



NRC Publications Archive Archives des publications du CNRC

Photophysics of fluorene copolymers : Control of fluorescence and charge separation by the presence of carbazole, oxadiazole, or biphenyl units

de Miguel, Maykel; Ferrer, Belén; Teruel, Laura; Garcia, Hermenegildo; Jin, Yinan; Li, Yuning; Ding, Jianfu

This publication could be one of several versions: author's original, accepted manuscript or the publisher's version. / La version de cette publication peut être l'une des suivantes : la version prépublication de l'auteur, la version acceptée du manuscrit ou la version de l'éditeur.

For the publisher's version, please access the DOI link below. / Pour consulter la version de l'éditeur, utilisez le lien DOI ci-dessous.

Publisher's version / Version de l'éditeur:

<https://doi.org/10.1021/jp900556z>

The Journal of Physical Chemistry C, 113, 9, pp. 8471-8477, 2009-04-21

NRC Publications Record / Notice d'Archives des publications de CNRC:

<https://nrc-publications.canada.ca/eng/view/object/?id=2242d56b-2b8a-4a11-9bff-a2970a355c89>

<https://publications-cnrc.canada.ca/fra/voir/objet/?id=2242d56b-2b8a-4a11-9bff-a2970a355c89>

Access and use of this website and the material on it are subject to the Terms and Conditions set forth at

<https://nrc-publications.canada.ca/eng/copyright>

READ THESE TERMS AND CONDITIONS CAREFULLY BEFORE USING THIS WEBSITE.

L'accès à ce site Web et l'utilisation de son contenu sont assujettis aux conditions présentées dans le site

<https://publications-cnrc.canada.ca/fra/droits>

LISEZ CES CONDITIONS ATTENTIVEMENT AVANT D'UTILISER CE SITE WEB.

Questions? Contact the NRC Publications Archive team at

PublicationsArchive-ArchivesPublications@nrc-cnrc.gc.ca. If you wish to email the authors directly, please see the first page of the publication for their contact information.

Vous avez des questions? Nous pouvons vous aider. Pour communiquer directement avec un auteur, consultez la première page de la revue dans laquelle son article a été publié afin de trouver ses coordonnées. Si vous n'arrivez pas à les repérer, communiquez avec nous à PublicationsArchive-ArchivesPublications@nrc-cnrc.gc.ca.



Photophysics of Fluorene Copolymers: Control of Fluorescence and Charge Separation by the Presence of Carbazole, Oxadiazole, or Biphenyl Units

Maykel de Miguel, Belén Ferrer, Laura Teruel, and Hermenegildo García*

Instituto de Tecnología Química CSIC-UPV and Departamento de Química, Universidad Politécnica de Valencia, Camino de Vera s/n, 46022 Valencia, Spain

Yinan Jin, Yuning Li, and Jianfu Ding*

Institute for Chemical Process and Environmental Technology, National Research Council Canada, 1200 Montreal Road, Ottawa, Ontario K1A 0R6, Canada

Received: January 19, 2009; Revised Manuscript Received: March 23, 2009

A set of fluorene copolymers designed to introduce electron donor/acceptor structures in the polymer chain that could eventually produce more efficient charge separation with long lifetimes has been prepared. To validate our approach, herein we report photoluminescence and laser flash photolysis measurements of the series of alternating specially functionalized fluorene copolymers. The copolymers contain 9,9-dioctylfluorene and *N*-octylcarbazole, oxadiazole, and oxadiazole–octafluorobiphenyl–oxadiazole units. It appears that the copolymer with the longest charge separated state lifetime and the highest charge separation quantum yield of the series is an alternating copolymer of a *N*-octylcarbazole and trifluorene units in which two fluorenes were attached with hydroxyhexyl side groups and the central fluorene with octyl side group at C-9 positions, respectively. These photophysical data suggest that this polymer a good candidate for photovoltaic cell and polymer light-emitting diode applications.

Introduction

Conjugated polymers with various structures have attracted considerable attention due to their important applications in polymeric light-emitting diodes (PLEDs), organic photovoltaic cells (PVCs), and field-effect organic transistors (FETs).^{1–5} During the recent years, polyfluorenes, including fluorene homo- and copolymers, have become promising emitters to be utilized in the fabrication of commercial PLEDs. Among the advantages of polyfluorenes for these applications, the most important ones are their high photoluminescence (PL) and electroluminescence (EL) efficiency, excellent thermal and oxidative stability, and their good solubility in common organic solvents.^{6–8} Polyfluorenes are among the best performing blue light emitters due to their large band gap.^{9,10} To improve their optoelectronic properties, there is a continuous interest to synthesize suitably modified polyfluorenes for nanotechnology.^{11,12}

Herein, electron-donating unit, carbazole, and strong electron-withdrawing units, octafluorobiphenyl and oxadiazole, have been included into the polyfluorene chain to introduce electron donor and/or acceptor sites that could lead to an enhanced charge separation quantum yield and to long lifetimes of this transient state.

Efficient charge separation and introduction of robust units can also serve to alleviate polyfluorene degradation that still represents a major limitation on the commercial application of these polymers.^{13,14} Upon charge separation, the transient species formed in fluorene homopolymer are highly vulnerable to the attack by water and oxygen, which cause a deterioration of the polymer performance. The ultimate factor controlling degradation is the high reduction and oxidation potential of the polymer

due to the energy of HOMO and LUMO, respectively. These energies can be adjusted by placing special units in the polymer that after trapping electrons and holes form more stable species. Our approach of preparation of fluorene copolymers can serve to obtain materials with enhanced performance for PLEDs and PVCs.

In this context, we have prepared a set of fluorene copolymers that have been specially designed for efficient charge separation. This efficiency can be demonstrated by data of quantum yield and lifetimes of charge separation and could eventually be reflected in higher polymer stability.

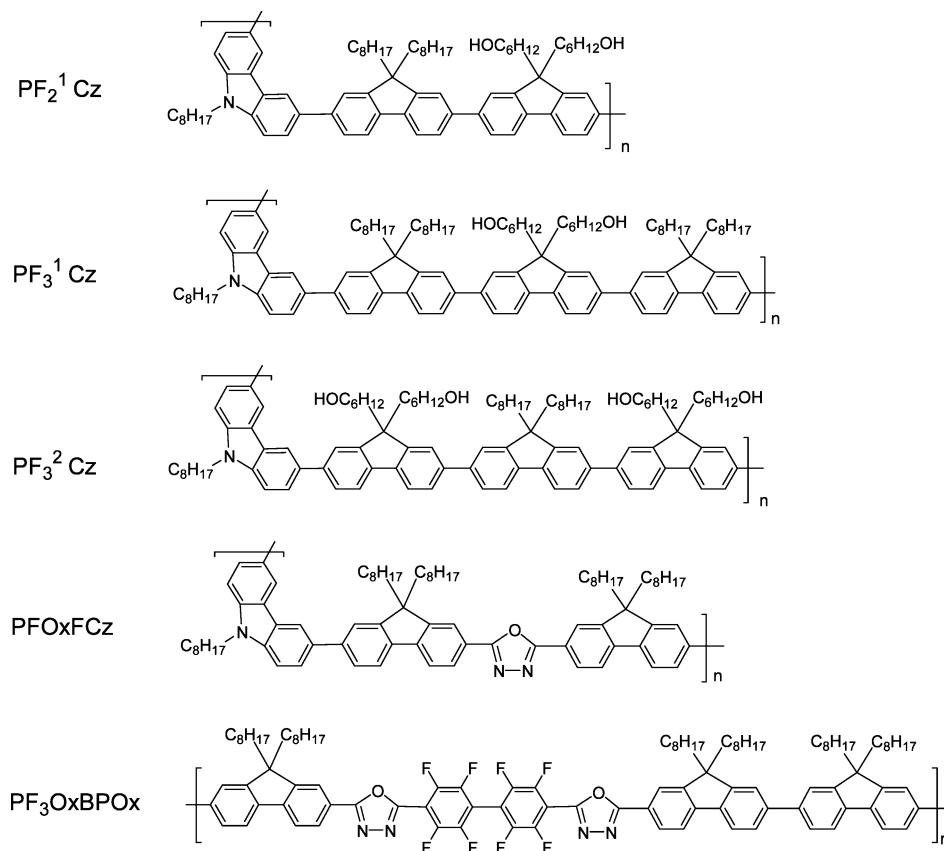
Herein we report photoluminescence and laser flash photolysis measurements of a series of alternating copolymers based on 9,9-dioctylfluorene (F) and octylcarbazole (Cz), oxadiazole (Ox), and oxadiazole–octafluorobiphenyl–oxadiazole (OxBPOx) units. The comonomer units have been selected based on their ability to form stable radical ions that can act as trapping sites for charge separated state. In addition, it can be anticipated that the presence of octyl side chains will favor the solubility of the polymers in conventional organic solvents, facilitating their processability. Also, the presence of OH group at the end of hydroxyhexyl side chains can serve eventually to increase the affinity of the polymers for metal oxide semiconductors and, particularly, for titania nanoparticles. Solubility and affinity for metal oxide semiconductors are two suitable properties facilitating processability and their use in PVC. The structures of the polymers under study are shown in Scheme 1.

Results and Discussion

The experimental part, including the description of the synthesis procedures, the materials, and techniques employed, is in the Supporting Information.

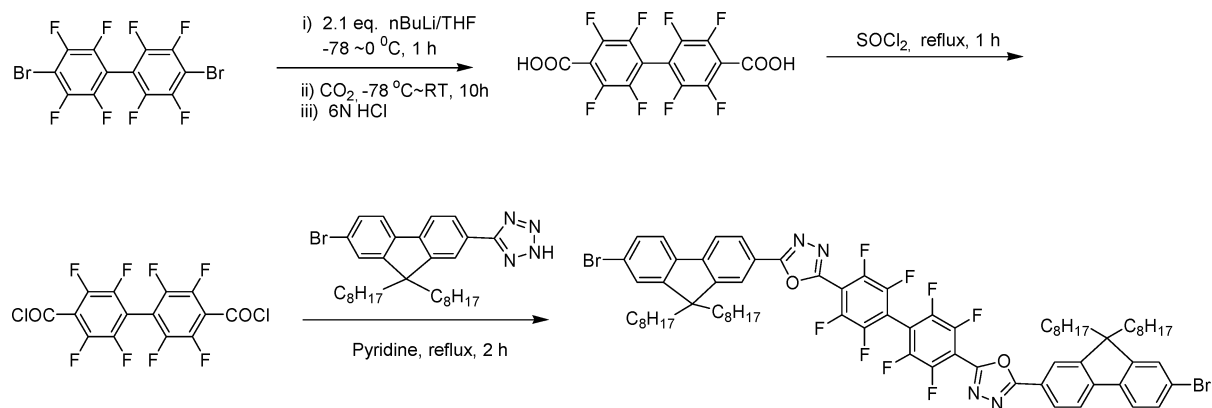
Materials Synthesis. The preparation of the dibromide of OxBPOx monomer, 4,4'-bis(7-bromo-9,9-dioctylfluorenyloxa-

* To whom correspondence should be addressed. E-mail: hgarcia@qim.upv.es (H.G.); jianfu.ding@nrc-cnrc.gc.ca (J.D.).

SCHEME 1: Chemical Structure of the Fluorene Copolymers under Investigation^a

^a The terms used to denote the copolymers indicate the monomers forming the structure (F: fluorene, Cz: carbazole, Ox: oxadiazole, BP: biphenyl) and the subscripts indicate the number of these units. The superscript refers to the fluorenyl units having hydroxyhexyl groups.

SCHEME 2: Reaction Route for the Preparation of 4,4'-Bis(7-bromo-9,9-dioctylfluorenyloxadiazolyl)octafluorobiphenyl



diazolyl)octafluorobiphenyl, as outlined in Scheme 2, was started from 4,4-dibromo-octafluorobiphenyl. It was easily converted to the dicarboxylic acid by lithiation followed by reacting with CO₂. This reaction is almost quantitative, and the ¹⁹F NMR showed no impurities in the crude product. The purified dicarboxylic acid was then reacted with the tetrazole compound to form the final monomer through a two-step reaction without purifying the intermediate.

The polymerization procedures used for the preparation of this series of copolymers (outlined in Scheme 1) are essentially the same as those previously used for the preparation of oxadiazole/fluorene,¹⁶ carbazole/fluorene,⁸ and triphenylamine/fluorene alternating copolymers¹⁵ using the Suzuki coupling technique. 6-Hydroxyhexyl groups have been introduced into the OH-functionalized carbazole/fluorene polymers by attaching

to the C-9 position of one or two of the fluorene units in every repeat unit. The presence of these hydroxyl groups on the side chain is clearly evident from the ¹H NMR spectra of P(F₂¹Cz), P(F₃¹Cz), and P(F₃²Cz) in Figure 1 in which the peaks at 3.52 ppm can be assigned to the protons on the carbon adjacent to the OH group. The area ratio of this peak to the ones at 4.40 and 2.13 ppm, ascribed to the protons on the first alkyl carbon adjacent to the N position of the carbazole unit and the C-9 position of the fluorene unit, is 2.00:1.00:3.95 for P(F₂¹Cz), 2.00:1.00:5.90 for P(F₃¹Cz), and 2.00:1.00:5.80 for P(F₃²Cz), respectively, which are in excellent agreement with their chemical structures.

Although the NMR signals in the aromatic region (7.5–8.5 ppm) for the OH-functionalized carbazole/fluorene polymers are overlapped, the peak of protons at the ortho and meta positions

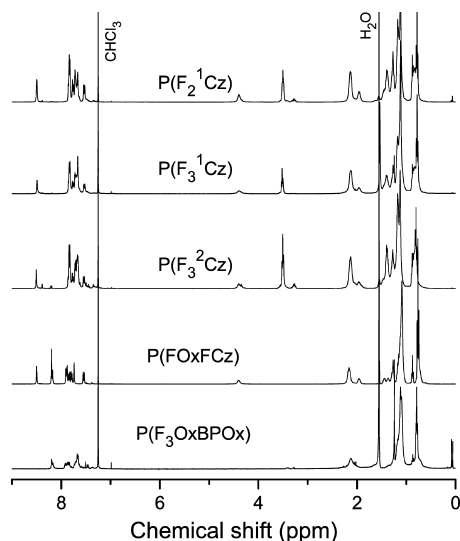


Figure 1. ^1H NMR spectra of the copolymers recorded in CDCl_3 .

TABLE 1: Molecular Weights and Thermal Analysis of the Fluorene Copolymers Studied in This Work

copolymer	M_w (Da)	M_w/M_n	T_g ($^\circ\text{C}$) ^a	T_d ($^\circ\text{C}$) ^b
P(F_2^1Cz)	23600	3.04	114.3	398.4
P(F_3^1Cz)	97000	4.70	119.1	419.5
P(F_3^2Cz)	10800	2.13	112.8	423.0
P(FOxFCz)	36900	1.78	143.3	423.0
P(F_3OxBPOx)	337000	12.5	138.4	359.5

^a Glass transition temperature taken from the second heating scan in DSC. ^b Decomposition temperature at 5% weight loss from TGA.

to the nitrogen of the carbazole unit at 8.50 and 7.54 ppm are well resolved. The ratio of the integration intensity of these two peaks to the sum of all the other aromatic protons is well in agreement with the structure. The NMR signals of P(FOxFCz) in the whole region are well resolved and can be assigned very well. However, the NMR spectrum of P(F_3OxBPOx) is relatively poor in quality. Some unknown weak signals were observed in the aromatic region. Considering the relative low solubility and the very high molecular weight and wide molecular weight distribution of this polymer (see Table 1), we propose that this polymer was lightly cross-linked during the polymerization and those unknown signals might be related to the cross-linked structure. Nevertheless it is noteworthy to remark that in general the NMR spectrum of this polymer is almost identical to that of P(F_3Ox) reported in literature,¹⁶ which has an analogous structure except the OxBPOx unit was replaced by Ox unit, indicating that the polymer has the designed structure.

Thermal Properties. The DSC analysis showed the polymers have a moderate glass transition temperature (T_g) in the range of 110–150 $^\circ\text{C}$. The data listed in Table 1 indicate the hydroxyl groups in the side chain have a slight effect on the T_g of the polymers, which is about 10 $^\circ\text{C}$ higher than the polymers with all octyl groups as side chain.⁸ However, P(F_3^2Cz) is exceptional. It has a lower T_g than P(F_3^1Cz), while its OH content is double of the later. This behavior can be attributed to the much lower molecular weight of P(F_3^2Cz). All the polymers excepting P(F_3OxBPOx) have a high thermal stability, with the onset of the decomposition temperature about 400 $^\circ\text{C}$. P(F_3OxBPOx) showed a slightly low thermal stability with a T_d of 359.5 $^\circ\text{C}$. A careful observation on its TGA curve revealed a slight weight loss for temperatures higher than 200 $^\circ\text{C}$. The DSC curve also showed a small exothermal peak with the maxima at 234 $^\circ\text{C}$.

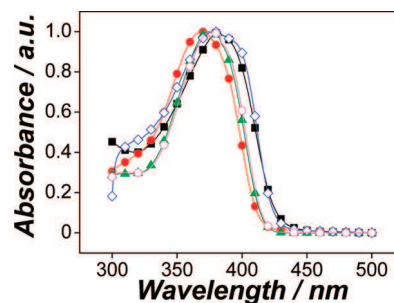


Figure 2. Normalized UV–visible absorption spectra of benzonitrile solutions of the copolymers: P(F_2^1Cz) (red filled circles), P(F_3^2Cz) (green filled triangles), P(F_3^1Cz) (red open circles), P(FOxFCz) (blue open diamonds), and P(F_3OxBPOx) (black filled squares).

By comparing the highly stable thermal property of the analogous fluorene/oxadiazole copolymer,¹⁶ we suggest that this lower stability is due to the very strong electron withdrawing property of the octafluorobiphenyl unit, which causes the adjacent oxadiazole unit to be less stable. This assumption is confirmed by the appearance of a broad exothermal peak starting at 215 $^\circ\text{C}$ of the corresponding monomer, 4,4'-bis(7-bromo-9,9-dioctylfluorenyloxadiazolyl)octafluorobiphenyl.

UV–Visible Absorption. The purpose of this work is to illustrate how possible it is to control the efficiency of photoinduced charge separation and the lifetime of these transient states by varying the structure of fluorene copolymers introducing suitable comonomers that can act as electron donor or electron acceptor termini. To demonstrate this methodology, we have started by recording the optical spectra of the polymers and their photoluminescence to subsequently perform laser flash photolysis that is the adequate photochemical technique to detect and characterize transient species. Thus, we will first comment on the optical spectroscopy.

As expected, in view of the presence of octyl chains, the copolymers prepared in this work except P(F_3OxBPOx) are easily soluble in THF, chlorobenzene, and dichlorobenzene. Moreover, the five copolymers under investigation are totally soluble in benzonitrile that appears as the solvent of choice for the study. The lowest solubility of P(F_3OxBPOx) can be rationalized by its slightly cross-linked structure as mentioned above, but a good solubility can be easily obtained by ultrasonically the solution for a couple of minutes.

The normalized UV–visible absorption spectra of the benzonitrile solutions of the five copolymers are shown in Figure 2.

One unstructured absorption band peaking below 400 nm was observed for the spectra of the five copolymers studied. In accordance with an elongated rodlike conformation containing predominantly only a single polymer chain, fluorene homopolymer in dilute THF solution exhibits an unstructured absorption spectrum with a maximum centered at 390 nm.¹⁷ The blue-shifted absorption of the five copolymers as compared to that of the fluorene homopolymer reflects the influence of copolymer composition on the frontier orbitals and/or a decrease in the conjugation length.

The OH-functionalized carbazole/fluorene copolymers are the ones which presented the shortest wavelength absorption. The λ_{max} of the absorption bands of these three polymers are 368, 374, and 374 nm for P(F_2^1Cz), P(F_3^2Cz), and P(F_3^1Cz), respectively. We can observe that the λ_{max} is somewhat red-shifted when increasing the fluorene segment length due to the low conjugation of the 3,6-carbazole unit, while the change in the number of OH groups does not apparently affect this value.

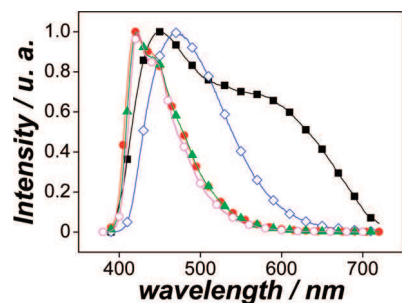


Figure 3. Photoluminescence spectra of N_2 -purged benzonitrile solutions of the copolymers (5×10^{-5} M): P(F_2^1Cz) (red filled circles, $\lambda_{ex} = 368$ nm), P(F_3^2Cz) (green filled triangles, $\lambda_{exc} = 374$ nm), P(F_3^1Cz) (red open circles, $\lambda_{ex} = 374$ nm), P(FOxFCz) (blue open diamonds, $\lambda_{ex} = 379$ nm), and P($F_3OxBPOx$) (black filled squares, $\lambda_{ex} = 385$ nm).

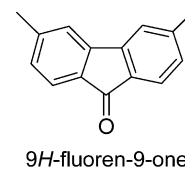
P(FOxFCz) shows a λ_{max} at 379 nm. Therefore, the introduction of an oxadiazole unit into the carbazole/fluorene copolymer causes a shift to a longer wavelength. This red-shift in λ_{max} could reflect an increase in the polymer conjugation due to the presence of push/pull units.

P($F_3OxBPOx$) shows the longest λ_{max} of the copolymers studied, peaking at 385 nm. The main difference with respect to the other copolymers is the absence of carbazole units and the presence of an oxadiazole–octafluorobiphenyl–oxadiazole unit. This phenomenon indicates the OxBPOx unit in the polymer has a higher conjugation than the 3,6-carbazole unit, having a similar effect as that reported for the oxadiazole unit.¹⁶ According to λ_{max} , the band gap energy of this copolymer is the most similar in the series to that of the fluorene homopolymer ($\lambda_{max} = 390$ nm) in spite of having structural units that can serve to modify the photophysical response of the material.

Photoluminescence Measurements. The photoluminescence spectra of the N_2 -purged benzonitrile solutions of the five copolymers studied are shown in Figure 3. The corresponding excitation spectrum for each copolymer is shown in the Supporting Information. It was observed that in all cases the excitation spectrum matches perfectly with the absorption spectrum except for the polymer P($F_3OxBPOx$). The photoluminescence spectra of the three carbazole/fluorene copolymers, P(F_x^yCz), exhibit a vibrational structure. On the basis of the behavior of the fluorene homopolymer,¹⁸ the three features centered at about 420, 445, and 475 nm are assigned to the $0 \leftarrow 0$, $1 \leftarrow 0$, and $2 \leftarrow 0$ intrachain singlet transitions in the copolymer chains. These photoluminescence spectra of P(F_x^yCz) polymers only show a very weak emission tail expanding to the green–orange region. This tail is observed for the fluorene homopolymer and based on the literature can be attributed to the contribution of two different phenomena: on the one hand to a dipole transition in the keto-defect units^{19,20} and on the other to an increase of the interchain interactions.²¹ It has been reported that oxidized chains of fluorene homopolymer, due to the spatial distribution of keto-defects units, have an absorption band extending into the green spectral region.¹³ The oxidation of the fluorene backbone introduces oxidized defects with 9*H*-fluoren-9-one structure (see below), which produce a breaking of the symmetry and conjugation of the polymer chain.

The photoluminescence spectra of the P(FOxFCz) and P($F_3OxBPOx$) do not present any vibronic structure, and the band has a much broader width at half-height as compared to the fluorene homopolymer and the OH-functionalized carbazole/fluorene copolymers.

Importantly, the emission of P($F_3OxBPOx$) exhibits two distinctive maxima, one at around 450 nm and the other at 600



nm. As it can be seen in the Supporting Information, Figure SI.1, the emission at 600 nm comes from an absorption centered at 385 nm, which matches with the absorption spectrum, while the emission at 450 nm comes from an absorption centered at 335 nm. The intense red-light dominant emission in the photoluminescence spectrum of P($F_3OxBPOx$) suggests that the photoluminescence emission of the copolymer is dominated by the OxBPOx units or to the occurrence of strong exciplex emission due to the association of donor–acceptor units of the polymer.

In any case, the red-light emission of P($F_3OxBPOx$) illustrates the potential of our approach to synthesize modified polyfluorenes having suitable units to alter the photophysical properties of these conducting polymers.

The emission lifetimes for the five copolymers under investigation obtained from the best fitting of the emission decay to single or double [case of P($F_3OxBPOx$)] exponential kinetics are shown in Table 2.

The carbazole/fluorene copolymers present the shortest emission lifetime. The introduction of different moieties in the polyfluorene structure makes somewhat longer the emission lifetime. It is interesting to note that the emission lifetime of the four copolymers containing a carbazole unit fits well to a single-exponential decay. However, when OxBPOx units are incorporated into the polyfluorene backbone, the emission decay at 600 nm presents two exponential contributions: the major component (τ 1.65 ns) has a similar lifetime to that measured for the rest of the copolymers and for the emission band at 450 nm, but the minor component has a considerably longer lifetime (8.28 ns). This longer emission lifetime could be attributed to the emission from an exciplex. Typically exciplex emission lacks vibrational structure, occurs at a longer wavelength than that of the excited molecule, and decays with a longer lifetime.²² These three features concur in the 600 nm emission of P($F_3OxBPOx$). Excimer could be formed from the inter- or intrachain interaction of electronically complementary units in the polymer. The fact that the emission of P($F_3OxBPOx$) is so different from those of the other members of the series reveals the strong influence of the OxBPOx structure on the photophysical properties. The presence of this unit in the polymer chain significantly promoted the chain interaction.

The fluorescence quantum yield, ϕ_f , of the five copolymers under study has also been measured by comparing the emission intensity with optically matched benzonitrile solutions of 2,4,6-triphenylpyrylium tetrafluoroborate as reference. 2,4,6-Triphenylpyrylium tetrafluoroborate is a dye that absorbs from 360 to 430 nm, presents intense emission at 470 nm, and has been previously used as fluorescence standard.²³ The procedure for determining ϕ_f has been included in the Supporting Information, and the obtained ϕ_f are reported in Table 2.

As it can be seen in Table 2, three of the copolymers containing a carbazole unit, P(F_3^2Cz), P(F_2^1Cz), and P(FOxFCz), exhibit a ϕ_f close to 1. This suggests that the three copolymers can be suitable for applications based on photoluminescence as in PLEDs, for which high fluorescence quantum yields are highly recommended.²⁴

The reason why P(F_3^1Cz) behaves differently with noticeable lower ϕ_f is unclear at the moment, and it is unlikely that the

TABLE 2: Emission Lifetimes of the N₂-Purged Benzonitrile Solutions (5 × 10⁻⁵ M) and Fluorescence Quantum Yields of the Copolymers under Study Measured by Taking 2,4,6-Triphenylpyrylium Tetrafluoroborate as the Standard (φ_f = 0.52)

copolymer	λ _{exc} (nm)	λ _{exc} (nm)	emission lifetime (ns)	φ _f
P(F ₃ ¹ Cz)	374	420	1.10	0.30
P(F ₃ ² Cz)	374	420	1.25	> 0.95
P(F ₂ ¹ Cz)	368	420	1.34	> 0.95
P(FO _x FCz)	379	470	2.14	> 0.95
P(F ₃ O _x BPO _x)	385	450	1.72	0.07
		600	1.65 (93%); 8.28 (8%)	

low φ_f is due to the presence of side OH groups that is the only difference with P(F₃²Cz). It seems more reasonable that differences in intra/inter-chain polymer conformation and aggregation causes a higher level of self-quenching of the emission in P(F₃¹Cz) that does not occur in the other members of the series. In this regard, the much higher molecular weight of this polymer as shown in Table 1 might be the major reason, which could cause stronger interaction between polymer chains, suggesting that it can be an optimum in the average molecular weight of the polymer to achieve the maximum in the emission quantum yield.

The structural O_xBPO_x units that cause the remarkable red-shift on the emission band, and the longest emission lifetime, are apparently also responsible for the very low φ_f. All these photoluminescence properties of P(F₃O_xBPO_x) point to the possibility that charge transfer association between electron-rich and electron-poor subunits of the copolymer both in the ground and excited state is controlling the behavior of this copolymer. If this is the case, laser flash photolysis could detect the photogeneration of charge separation.

Laser Flash Photolysis. The nature of the transient excited states and the ability of the polymers to generate charge separated states have been investigated by laser flash photolysis measurements of the five copolymers under study.

Upon 355 nm laser excitation of deaerated benzonitrile solutions, intense transient absorption spectra were recorded for the five copolymers. The main spectral features of these transient absorption spectra were also similar. They show a bleaching of the ground-state absorption between 340 and 410 nm, peaking at about 370 nm, together with a broad absorption band from 410 to 600 nm having a tail increasing in absorbance at 700 nm. As an example, Figure 4 shows the transient absorption spectra plotted as the relative variation of the signal intensity at a given time with respect to the initial signal (ΔJ/J₀) recorded at different times after 355 nm laser excitation of a benzonitrile

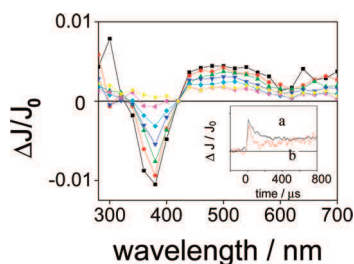


Figure 4. UV-visible transient absorption spectra of a N₂-purged benzonitrile solution of P(F₃²Cz) copolymer recorded 0.1 (black filled squares), 4 (red filled circles), 20 (green filled triangles), 50 (blue filled triangles), 100 (blue filled diamonds), 300 (red filled triangles), and 700 (yellow filled triangles) μs after 355 nm laser excitation. The inset shows the decay of the signals monitored at 500 (a) and 640 (b) nm.

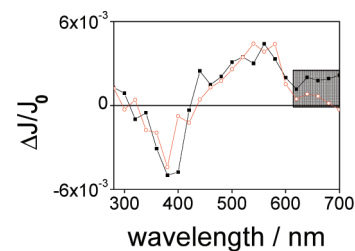
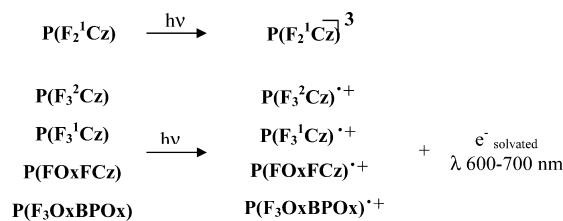


Figure 5. UV-visible transient absorption spectra of a N₂ (black filled squares) and O₂ (red open circles) purged benzonitrile solution of the copolymer P(F₃O_xBPO_x) recorded 0.1 μs after 355 nm laser excitation. Note that oxygen decreases significantly the absorption in the 600–700 nm region corresponding to solvated electrons.

SCHEME 3: Rationalization of the Transient Spectra of Fluorene Copolymers as Corresponding to Either the Electronic Triplet Excited State of Electron and Holes



solution of copolymer P(F₃²Cz). The decay kinetics of four out of the five copolymers follow the same trend and were different from that of P(F₂¹Cz) that exhibits a distinctive behavior. Thus, except for P(F₂¹Cz), the decays of the signals monitored at 500 and 640 nm for the rest of the copolymers are different, indicating that they correspond at least to two different species. The inset of Figure 4 shows the decays of the signals monitored at 500 and 640 nm, which serves to illustrate the two different decay kinetics observed for the four copolymers.

The four copolymers also show a common behavior in the presence of dissolved oxygen. Thus, all the polymers, except P(F₂¹Cz), undergo complete quenching of the transient absorption at λ_{max} 640 nm upon oxygen purging and partial quenching of the transient absorption at λ_{max} 500 nm. Under oxygen atmosphere, there is still transient absorption at 500 nm but the absorption at 640 nm has totally disappeared. To illustrate the influence of oxygen, Figure 5 shows the transient absorption spectrum recorded at the same delay time for a benzonitrile solution of copolymer P(F₃O_xBPO_x) under N₂ and O₂ atmosphere. On the basis of the optical spectrum of solvated electrons^{25,26} and its quenching behavior, we have assigned the absorption in the 600–700 nm region to solvated electrons in benzonitrile. To be consistent with the generation of electrons, the absorption in the 410–600 nm region and centered at 500 nm should be assigned to the positively charged electron hole on the polymer backbone. Scheme 3 summarizes the proposal.

Importantly, after oxygen quenching, the positively charged electron hole located on the polymer is significantly longer lived, indicating that charge recombination of electrons and holes is one of the prevalent deactivation pathways. Charge annihilation is obviously not possible when oxygen quenches the photoejected electrons.

The results obtained constitute a firm evidence in support of the occurrence of photoinduced charge separation upon light excitation of these copolymers.

The behavior of the copolymer P(F₂¹Cz) is notably different from that of the rest of copolymers. This specific photophysical behavior is unexpected because P(F₂¹Cz) has an analogous structure of P(F₃²Cz) and P(F₃¹Cz) copolymers. Thus, even

though the main spectral features of the transient absorption recorded after 355 nm laser excitation are similar to those of the copolymers P(F₃²Cz) and P(F₃¹Cz), previously commented, i.e., a bleaching of the ground-state absorption between 340 and 410 nm and a broad absorption band from 410 to 600 nm, as can be seen in Figure 6, there is an important difference in the transient absorption in the 600–700 nm region as well as in the quenching behavior by oxygen. Thus, it appears that no absorption attributable to solvated electrons appears in the 600–700 nm zone. In agreement with this, we notice that for P(F₂¹Cz), all the decays in the 400–700 nm range are coincident, indicating that the whole absorption band corresponds to the same species.

Moreover, this broad absorption band from 400 to 600 nm is completely quenched by oxygen in contrast to the lifetime increase observed under oxygen for the other four members of the series. The inset of Figure 6 shows the decay of the signal from P(F₂¹Cz) monitored at 500 nm under nitrogen and oxygen atmosphere. On the basis of the lack of solvated electron band and oxygen quenching of the 400–600 nm band, we have attributed this transient absorption band to the triplet excited state (Scheme 3).

Actually, a more detailed analysis of the transient decay at short time delays for the rest of the polymers shows that the triplet excited state claimed for P(F₂¹Cz) is also generated in the other four copolymers. As an example, for the copolymer P(F₃OxBPOx), the decay of the signal monitored at 500 nm is partially quenched by oxygen in a short time scale (<5 μs). However, as commented earlier, at a longer time scale, 800 μs, this transient decay is even shorter-lived under nitrogen compared to oxygen atmosphere. This increase in lifetime under oxygen is due to the scavenging of electrons by oxygen disfavoring geminate electron/hole recombination that is the major deactivation pathway for the 500 nm signal corresponding to electron holes.

On the basis of these observations, we can conclude that in the transient absorption band from 410 to 600 nm recorded for the copolymers P(F₃²Cz), P(F₃¹Cz), P(FOxFCz), and P(F₃OxBPOx), there is a minor contribution (about 15%), quantified based on the difference in the signal intensity immediately and 500 ns after the laser pulse, of the corresponding triplet excited-state at short delay times after the laser pulse. At longer time scales, this transient absorption band corresponds exclusively to the positively charged hole species, whose lifetimes increase in the presence of oxygen.

We have measured the lifetime of the charge separated states under N₂ atmosphere for the four different copolymers for which we have observed charge separation. The data have been obtained from the best fit of the decays monitored at 500 nm and long time scale to single or biexponential kinetics and are collected in Table 3.

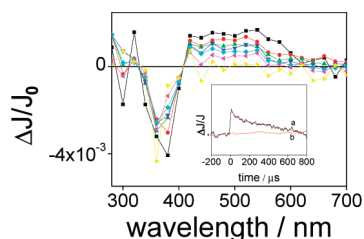


Figure 6. UV-visible transient absorption spectra of a N₂-purged benzonitrile solution of the copolymer P(F₂¹Cz) recorded 0.1 (■), 4 (●), 20 (▲), 50 (▲), 100 (■), 300 (▲) and 700 (▲) μs after 355 nm laser excitation. The inset shows the decay of the signal monitored at 500 nm under N₂ (a) and O₂ (b) atmosphere.

TABLE 3: Lifetime and Relative Quantum Yield of the Charge Separated State of the Copolymers under Investigation Measured from the Best Fit of the Decays Monitored at 500 nm to First Order or Two Consecutive First-Order Kinetics

copolymer	lifetime of the triplet excited state (μs)	lifetime of the charge separated state (μs)	φ _{cs} (%)
P(F ₂ ¹ Cz)	44.8	<i>a</i>	<i>a</i>
P(F ₃ ² Cz)	7.6	86.4	100
P(F ₃ ¹ Cz)	3.9	316.0	100
P(FOxFCz)	17.2	183.4	24
P(F ₃ OxBPOx)	3.6	37.3	31

^a No charge separation is observed.

In those cases where the decay monitored at 500 nm fits to a double first-order kinetics, it can be proposed that the shortest lifetime corresponds to the triplet excited state while the much longer component would correspond to the lifetime of the electron hole localized on the polymer. According to this, the charge separated states are very long-lived for those copolymers containing a carbazole unit. Actually, photogenerated charge separated state in copolymers P(FOxFCz) and P(F₃²Cz) does not decay completely in 800 μs, which is the longest time scale available for our nanosecond laser setup. Therefore, the introduction of an appropriate number of carbazole units in the polyfluorene structure can be useful for those applications in which charge separation has to lead to the target effect as in photovoltaics and PLED applications.

As commented before, the copolymer P(F₂¹Cz) behaves in a different way with respect to the other carbazole copolymers, and the lifetime collected on the Table 3 corresponds to the triplet excited state. The substitution of the carbazole unit by the octafluorobiphenyl unit, the case of the copolymer P(F₃OxBPOx), makes significantly shorter the lifetime of the charge separated state, 37.30 μs. This could be interpreted based on the previous literature data that has shown that carbazole radical cation is significantly more stable and longer lived than the radical cation corresponding to biphenyl.^{22,27,28}

Another important data for most applications is the relative efficiency of photoinduced charge separation. We have been able to measure the relative charge separation quantum yield, φ_{cs}, of the five copolymers under study by comparing the intensity of the transient absorption signals monitored at 640 nm corresponding to solvated electrons in the solvent, measured from benzonitrile solutions of the copolymers having the same absorbance at the laser excitation wavelength, 355 nm. Electrons are the common species for the four copolymers leading to charge separation, while the positively charged hole species, assigned to the transient absorption band centered at 500 nm, may have somewhat different molar absorptivity depending on the polymer backbone where this electron hole is photogenerated.

The data of the relative efficiency for charge separation is also given in Table 3. As can be seen, the φ_{cs} of copolymers P(F₃²Cz) and P(F₃¹Cz) is higher than the one of the copolymers P(F₃OxBPOx) and P(FOxFCz). It has to be commented that, however, the absolute φ_{cs} values should be small because, as Table 2 shows, the fluorescence quantum yields are very high and the sum of quantum yields of photophysical and photochemical processes should not exceed unity, φ_{fl} + φ_{isc} + φ_{ic} + φ_{cs} = 1. The experimental error on determining the fluorescence quantum yield derives mainly from the uncertainty in the integration of the emission curves.

Then, we can conclude that the carbazole and the OH-functionalized fluorene units are the best moieties for promoting

efficient charge separation in a fluorene copolymer. The oxadiazole and octafluorobiphenyl units are less appropriated with respect to those applications needing charge separation.

From the above laser flash photolysis data, it appears that the copolymer with the longest lifetime of the charge separated state and the highest charge separation quantum yield is P(F₃²Cz). These photophysical data of P(F₃²Cz) appear to be optimum for having a high performance in photovoltaic cells and PLED applications. Thus, the basic photophysical data should be useful in predicting properties and leading the synthesis of polyfluorenes for PVC and PLED applications.

Conclusions

In this article, fluorescence and photoinduced charge separation of a set of new fluorene copolymers were studied. Oxadiazole and octafluorobiphenyl moieties incorporated into the polyfluorene backbone causes the lowest efficiency of the emission, the appearance of a new red-shifted emission band, and the shortest lifetime of the charge separation with the lowest charge separation efficiency. In contrast, the presence of carbazole and the OH-functionalized fluorene moieties makes these fluorene copolymers more suitable for PVC and PLED applications because they cause the highest emission efficiency and promote efficient and long-lived charge separation.

Acknowledgment. Financial support by a joint Canadian-Spanish NRC-CSIC program and a R&D Project from the Spanish Ministry of Science and Education (CTQ200767805/PPQ) is gratefully acknowledged.

Supporting Information Available: Synthesis and characterization of the set of fluorene copolymers; fluorescence quantum yield determination; relative charge separation quantum yield, ϕ_{cs} , determination. This material is available free of charge via the Internet at <http://pubs.acs.org>.

References and Notes

(1) Burroughes, J. H.; Bradley, D. D. C.; Brown, A. R.; Marks, R. N.; Mackay, R. H.; Friend, R. H.; Burns, P. L.; Holmes, A. B. *Nature (London)* **1990**, *347*, 539.

(2) Gustafsson, G.; Cao, Y.; Treacy, G. M.; Klavetter, F.; Colaneri, N.; Heeger, A. J. *Nature (London)* **1992**, *357*, 477.

(3) Sariciftci, N. S.; Smilowitz, L.; Heeger, A. J.; Wudl, F. *Science* **1992**, *258*, 1474.

(4) Coakley, K. M.; McGehee, M. *Chem. Mater.* **2004**, *16*, 4533.

(5) Shrotriya, V.; Li, G.; Yao, Y.; Yang, Y. *J. Appl. Phys.* **2005**, *98*, 043704.

(6) Grice, A. W.; Bradley, D. D. C.; Bernius, M. T.; Inbasekaram, M.; Wu, W. W.; Woo, F. P. *Appl. Phys. Lett.* **1998**, *73*, 629.

(7) Fletcher, R. B.; Lidzey, D. G.; Bradley, D. D. C.; Walker, S.; Inbasekaram, M.; Woo, F. P. *Synth. Met.* **2000**, *111*, 151.

(8) Li, Y.; Ding, J.; Day, M.; Tao, Y.; Lu, J.; Diorio, M. *Chem. Mater.* **2004**, *16*, 2165.

(9) Pei, Q.; Yang, Y. *J. Am. Chem. Soc.* **1996**, *118*, 7416.

(10) Kulkarni, A. P.; Zhu, Y.; Jenekhe, S. A. *Macromolecules* **2005**, *38*, 1553.

(11) Liu, Q.-D.; Lu, J.; Ding, J.; Day, M.; Tao, Y.; Barrios, P.; Stupak, J.; Chan, K.; Li, J.; Chi, Y. *Adv. Funct. Mater.* **2007**, *17*, 1028.

(12) Ding, J.; Qi, Y. *Macromolecules* **2008**, *41*, 751.

(13) Biagioni, P.; Celebrano, M.; Labardi, M.; Polli, D.; Zavelani-Rossi, M.; Cerullo, G.; Lanazani, G.; Finazzi, M.; Duò, L. *Phys. Status Solidi* **2008**, *5*, 2587.

(14) Ranger, M.; Rondeau, D.; Leclerc, M. *Macromolecules* **1997**, *30*, 7686.

(15) Lu, J.; Jin, Y.; Ding, J.; Tao, Y.; Day, M. *J. Mater. Chem.* **2006**, *16*, 593–601.

(16) Ding, J.; Day, M.; Robertson, G.; Roovers, J. *Macromolecules* **2002**, *35*, 3474.

(17) Knaapila, M.; Garamus, V. M.; Dias, F. B.; Almsy, L.; Galbrecht, F.; Charas, A.; Morgado, J.; Burrows, H. D.; Scherf, U.; Monkman, A. P. *Macromolecules* **2006**, *39*, 6505.

(18) Yang, X. H.; Neher, D.; Spitz, C.; Zojer, E.; Bredas, J. L.; Günter, R.; Scherf, U. *J. Chem. Phys.* **2003**, *119*, 6832.

(19) Becker, K.; Lupton, J. M.; Feldmann, J.; Nehls, B. S.; Galbrecht, F.; Gao, D.; Scherf, U. *Adv. Funct. Mater.* **2006**, *16*, 364.

(20) Cadby, A.; Dean, R.; Fox, A. M.; Jones, R. A. L.; Lidzey, D. G. *Nano Lett.* **2005**, *5*, 223.

(21) Wu, C.; McNeill, J. *Langmuir* **2008**, *24*, 5855.

(22) Murov, S. L.; Carmichael, I.; Hug, G. L. *Handbook of Photochemistry*; Marcel Dekker: New York, 1993.

(23) Miranda, M. A.; Garcia, H. *Chem. Rev.* **1994**, *94*, 1063.

(24) Müllen, K.; Scherf, U. *Organic Light Emitting Devices*; Wiley-VCH: New York, 2006.

(25) Jou, F. Y.; Freeman, G. R. *Can. J. Chem.* **1979**, *57*, 591.

(26) Fletcher, J. W.; Seddon, W. A. *Faraday Discuss. Chem. Soc.* **1977**, *63*, 18.

(27) Ohkita, H.; Nomura, Y.; Tsuchida, A.; Yamamoto, M. *Chem. Phys. Lett.* **1996**, *263*, 602.

(28) Masuhara, H.; Itaya, A., *Dynamics and Mechanism of Photoinduced Electron Transfer and Its Related Phenomena*; Elsevier, Amsterdam, 1992.

JP900556Z